International Journal of Nanomedicine

Dovepress
open access to scientific and medical research

Open Access Full Text Article

ORIGINAL RESEARCH

Blood-Nanoparticle Interactions Create a Brain Delivery Superhighway for Doxorubicin

Zhuoxuan Li[1], Tatyana Kovshova[2], Julia Malinovskaya[2], Julian Knoll[1], Saeed Shanehsazzadeh[1], Nadezhda Osipova[2], Anastasia Chernysheva[3], Pavel Melnikov[2], Svetlana Gelperina[2], Matthias G Wacker[1]

[1]National University of Singapore, Department of Pharmacy and Pharmaceutical Sciences, Faculty of Science, Singapore; [2]Dmitry Mendeleev University of Chemical Technology of Russia, Moscow, Russia; [3]V. Serbsky Federal Medical Research Centre of Psychiatry and Narcology of the Ministry of Health of the Russian Federation, Moscow, Russia

Correspondence: Matthias G Wacker, Email matthias.g.wacker@nus.edu.sg

Purpose: This study investigated the brain targeting mechanism of doxorubicin-loaded polybutyl cyanoacrylate (PBCA) nanoparticles, particularly their interactions with the blood-brain barrier (BBB). The BBB protects the brain from drugs in the bloodstream and represents a crucial obstacle in the treatment of brain cancer.

Methods: An advanced computer model analyzed the brain delivery of two distinct formulations, Doxil® and surfactant-coated PBCA nanoparticles. Computational learning was combined with in vitro release and cell interaction studies to comprehend the underlying brain delivery pathways.

Results: Our analysis yielded a surprising discovery regarding the brain delivery mechanism of PBCA nanoparticles. While Doxil® exhibited the expected behavior, accumulating in the brain through extravasation in tumor tissue, PBCA nanoparticles employed a unique and previously uncharacterized mechanism. They underwent cell hitchhiking, resulting in a remarkable more than 1000-fold increase in brain permeation rate compared to Doxil® (2.59×10^{-4} vs 0.32 h^{-1}).

Conclusion: The nonspecific binding to blood cells facilitated and intensified interactions of surfactant-coated PBCA nanoparticles with the vascular endothelium, leading to enhanced transcytosis. Consequently, the significant increase in circulation time in the bloodstream, coupled with improved receptor interactions, contributes to this remarkable uptake of doxorubicin into the brain.

Keywords: BBB, brain targeting, CNS, modeling, doxorubicin, drug delivery

Introduction

Brain cancers include several primary and secondary tumors such as glioblastoma multiforme and brain metastases. Glioblastoma multiforme is one of the most aggressive cancers worldwide; it comes with an average survival of 12–15 months after diagnosis and a two-year survival rate of 25%.[1] Even more concerning, brain metastases from lung and breast cancers affect up to 200,000 patients per year.[2] Once a tumor spreads into the brain, the median survival under first-line treatment is 9.2 months only.[2] The blood-brain barrier (BBB) still poses a challenge in the treatment of brain cancer. It is created by the vascular endothelial cells in the brain that form tight junctions and inhibit the paracellular transport from blood circulation into the central nervous system (CNS). To date, most anticancer drugs cannot be delivered to the brain in sufficient quantity.[3–5] Nanomedicines such as liposomes and coated nanoparticles have been developed as a feasible strategy to deliver those therapeutical moieties to their target sites[4,6–8] (Figure 1A). Transporters can facilitate the selective uptake of therapeutical agents from the blood vessel into the brain. They include ion channels, carrier molecules, and receptor-initiated delivery through the formation of vesicles followed by transcytosis (Figure 1Bi).

Tumor growth together with neuroinflammation often leads to a local breakdown of the BBB that allows larger molecules and nanoparticles to enter the tumor site (Figure 1Bii).[4,6–9] As a consequence, nanoparticles, and liposomes have been developed that deliver their payload to malignant tissues in the brain. Although this localized uptake comes with higher selectivity for the tumor area, the invasive growth of the cancer cells into deeper tissues increases the

Received: 10 October 2023
Accepted: 9 January 2024
Published: 5 March 2024

Graphical Abstract

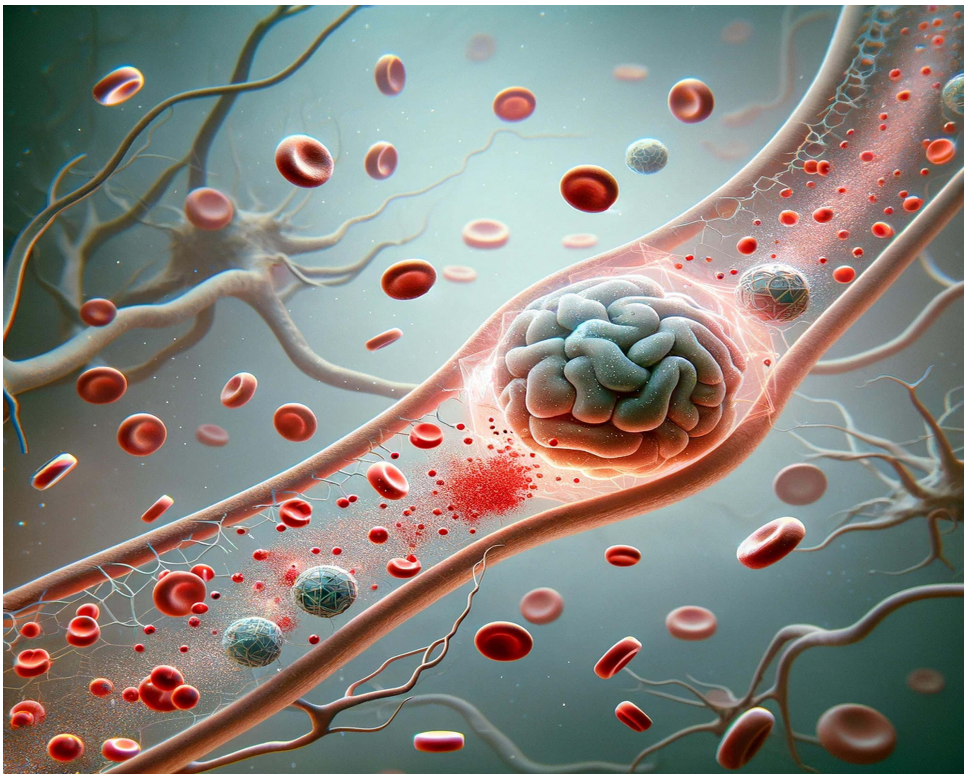

distance between the entry point of the drug and potential target sites. In a clinical setting, the size, morphology, and localization of tumors vary between different patients. Hence, most delivery strategies that rely on local extravasation such as long-circulating liposomal doxorubicin (Doxil®) often fail in clinical translation.[10] They are not able to access tumor cells in deeper tissues and mostly affect the side effects of drug therapy.[10] More successful strategies utilize receptor-mediated transcytosis of nanoparticles through the BBB (refer to Figure 1Biii).[11] The average distance between two blood vessels is approximately 40 µm.[8] Consequently, active transport enables rapid access to most tissues in the brain with much shorter diffusion pathways.[6] Common drug-targeting ligands include apolipoproteins,[6,11] transferrin,[12,13] and insulin.[14] However, the capacity of this transport mechanism is limited as well. Particularly nanomedicines with a high binding affinity for their receptor are often affected by lysosomal degradation.[14–16] Hence, high exposure of the vascular endothelium with the nanoparticles together with a moderate binding affinity to the target receptor is most favorable to ensure efficient transcytosis.[16]

Another important aspect to consider is the presence of efflux transporters such as the p-glycoprotein and ATP-dependent ABC transporters, which have an impact on a wide variety of drug molecules.[17,18] One example is doxorubicin, which is affected by these multidrug resistance transporters,[19] leading to efficient elimination of the drug from the brain. PBCA nanoparticles have been demonstrated to efficiently bypass these efflux pumps in various scenarios,[19–21] including the delivery of substances like dalargin, loperamide, and doxorubicin to the brain in vivo.[21–23] However, the precise mechanism by which the nanoparticles facilitate delivery remained unknown.

Here we describe a quantitative evaluation of the brain transport of doxorubicin following the administration of PBCA nanoparticles and pegylated liposomes. A novel computer model was developed followed by the evaluation of biodistribution studies in rats described in the literature.[24,25] This led to two surprising discoveries. Compared to liposomal delivery with Doxil®, the doxorubicin transport rate, a crucial indicator for the success of targeted delivery

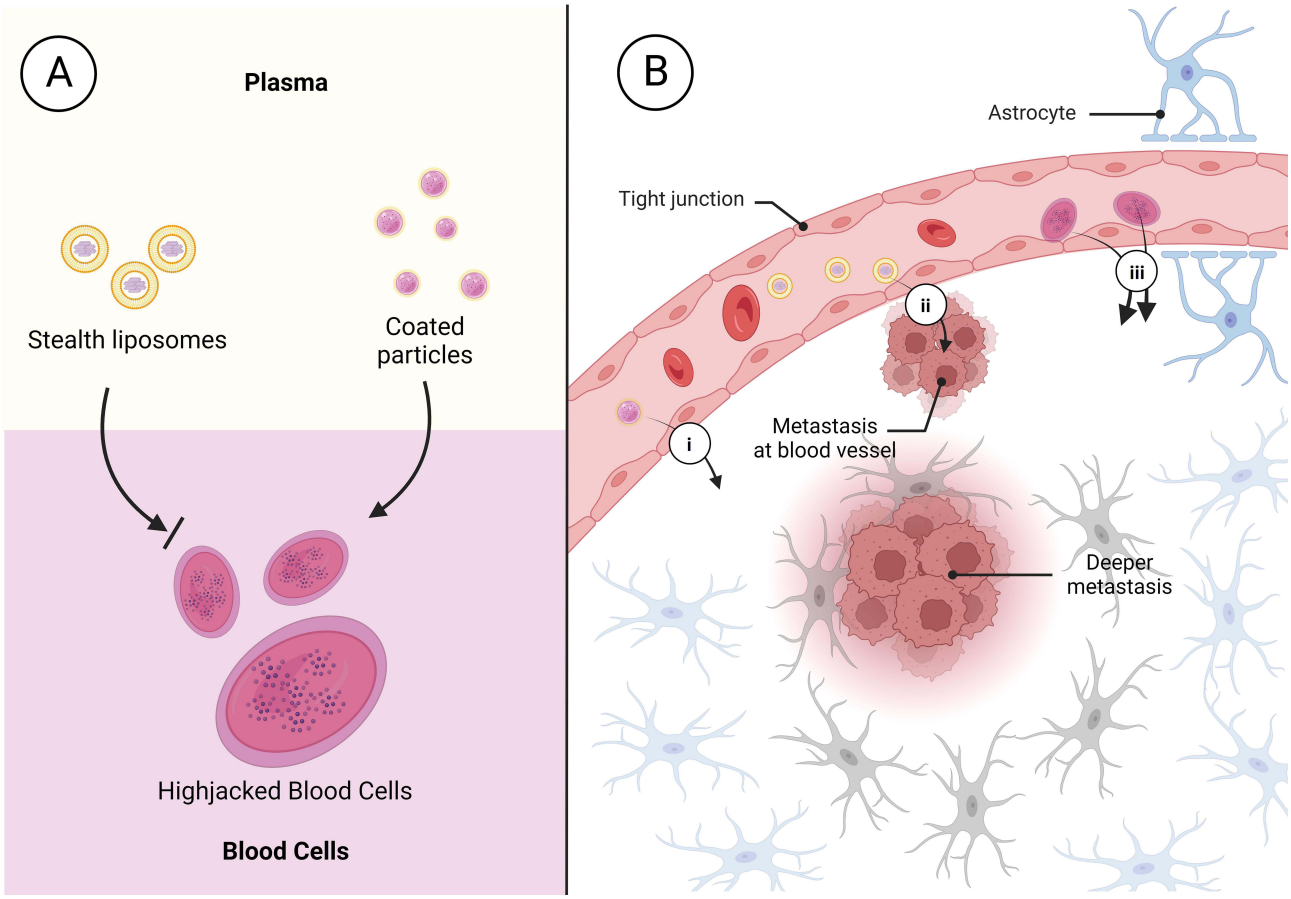

Figure 1 Possible ways for nanomedicines accessing to lesion locations in the brain. (**A**) Illustration of the mechanism of blood cell hitchhiking facilitated by surfactant-coated nanoparticles. Liposomes bind to blood cells to a much lower extent and do not utilize an active uptake mechanism. (**B**) Entry routes into the brain using (i) direct transporter-mediated transcytosis through interaction with the BBB, (ii) extravasation at the tumor site, and (iii) cell shuttling which facilitates receptor-mediated transcytosis. Cell hitchhiking increases the distribution of the drug into the brain significantly. Created with BioRender.com.

into the brain, increased over 1000-fold. Following a decrease in plasma concentration, there was a subsequent delay in the increase of doxorubicin concentration in the brain, which was previously misinterpreted by the authors two decades ago. Based on recent discoveries and supported by our in vitro investigations, we have substantiated the involvement of blood cells in targeted brain delivery.

Materials and Methods

Chemicals

Doxorubicin hydrochloride (98%) was purchased from Cayman Chemical (Michigan, USA) and n-butyl-2-cyanoacrylate monomer for the synthesis of PBCA nanoparticles was obtained from Shengjie Technology Co., Ltd (Jingzhou, Hubei, China). Cyanine 5.5 NHS ester was purchased from Lumiprobe Crop. (Cockeysville, Maryland, USA). The PTDR devices were kindly provided by Pharma Test Apparatebau AG (Hainburg, Germany). The instrument has been described in more detail previously (patent no. WO2015039749A1) and various applications related to this methodology have been reported.[11,25,26]

The cellulose ester (CE) dialysis membrane, with a molecular weight cut-off (MWCO) of 300 kDa, had specific dimensions: a flat width of 31 mm and a diameter of 20 mm. This membrane was procured from VWR-Singapore Pte Ltd (Singapore, Singapore).

Dulbecco's Modified Eagle Medium (high glucose) for cell culture was sourced from Thermo Fisher Scientific (Waltham, MA, USA). Fetal bovine serum (FBS) and Penicillin-Streptomycin (P/S) were acquired from GibcoTM (Paisley, Scotland). Plasmocin® was obtained from InvivoGen (San Diego, CA, USA). Various plastic cell culture

items such as dishes, plates, and flasks, along with Transwell® polycarbonate membrane cell culture inserts, were purchased from Corning Inc. (Lowell, MA, USA). Ethylenediaminetetraacetic acid (EDTA) was procured from Sigma-Aldrich (Darmstadt, Germany). Ultrapure water was generated using MilliQ Advantage (Merck, Kenilworth, New Jersey, USA). All remaining chemicals were either of analytical or high-performance liquid chromatography (HPLC) grade and were utilized without further modification.

Computer Model and Pharmacokinetic Analysis

The pharmacokinetic analysis was based on an extended version of the physiologically-based nanocarrier biopharmaceutics (PBNB) model.[24,25] Brain and tumor compartments as well as multiple related delivery pathways were added to further resolve the biodistribution of nanomedicines. All distribution and elimination processes were assumed to follow first-order kinetics and the drug was considered to be homogeneously distributed in each compartment. This corresponded to the quantification methods used to determine the drug content.[24,25] The model structure is an important outcome of this investigation and was therefore included in the results section.

The models were created using Monolix 2020R1 (Lixoft, Antony, France) and the Stochastic Approximation Expectation Maximization (SAEM) algorithm for parameter estimation.[27] A log-normal distribution of the population parameters was assumed. For model validation, the goodness-of-fit, observation-versus-prediction, and individual weighted residuals (IWRES) versus time plots were inspected.[28]

Modeling Biodistribution of Free Doxorubicin

The pharmacokinetic profiles of free doxorubicin were used to calculate the rate constants and volume of distribution (V_{DF}) involved in the biodistribution of the released drug. This includes the distribution rates into the periphery, brain, and tumor compartments (k_{Peri_in}, k_{Peri_out}, k_{B_in}, k_{B_out}, k_{T_in}, k_{T_out}) as well as the elimination rate constant (k_{e_plasma}) of doxorubicin.

Drug concentrations in the brain and tumor were reported in micrograms per gram of wet tissue (µg/g). For the brain, the physiological organ weight fraction of the total body weight (f_{brain}) was used to estimate these total amounts. The concentration in the tumor was calculated using the tumor weight observed with this animal model (W_{tumor}). The pharmacokinetic data sets used to model the behavior of free doxorubicin are summarized in Table S1. The population parameters of free doxorubicin were later used to model the biodistribution of nanomedicines.

Modeling Biodistribution of Nanomedicines

As a next step, we modeled the biodistribution of doxorubicin-loaded liposomes[24] and PBCA nanoparticles.[25] The distribution of the released drug was predicted using the population parameters identified for the free drug (refer to Modeling Biodistribution of Free Doxorubicin).

Nanomedicines exhibit limited mobility in the vascular system. Hence, the volume of distribution of the encapsulated drug (V_{DC}) corresponds to the physiological plasma volume of rats.[11,28,29] From the vascular (central) compartment, the delivery system is distributed through four alternative pathways. They include the accumulation of the delivery system ($t_{1/2}$) as well as the drug release which is reflected by the release rate constant (k_r). To define initial estimates for the carrier half-life ($t_{1/2}$), a non-compartmental analysis of the total plasma pharmacokinetics was conducted using Pkanalix 2020R1 (Lixoft, Antony, France). Based on the clearances of Doxil® and PBCA nanoparticles and defining a variation of at least 30%, the half-lives of 35–40.12 h^{-1} for Doxil® and 0.398–8.74 h^{-1} for PBCA nanoparticles were selected, respectively.

The two other pathways involve direct interactions with the respective target organs including the brain (k_{targB}) and the tumor tissue (k_{targT}). As the pharmacokinetic studies using PBCA nanoparticles were conducted in healthy animals, the tumor compartment was included solely to estimate the population parameters of Doxil®. The initial estimates and parameter ranges are summarized in the Tables S2.

Synthesis of Poly(Butyl Cyanoacrylate) Nanoparticles

Doxorubicin-loaded poly(butyl cyanoacrylate) (PBCA) particles were prepared by anionic emulsion polymerization.[25] Briefly, a volume of 100 µL of the monomer n-butyl-2-cyanoacrylate was added to 10 mL of a 1% (m/v) dextran solution

in 0.01 N HCl under constant stirring (400 rpm) at ambient temperature. A 2.5% doxorubicin solution was added to the mixture after 5 min to obtain a final doxorubicin concentration of 0.25% (m/v). For fluorescent labeling of the PBCA nanoparticles, cyanine 5.5 (Cy5.5) was added to the suspension in the PBCA-Cy5.5 ratio of 2000:1 and stirred for 3 h. The polymerization was completed by neutralization with 0.1 N sodium hydroxide, followed by stirring for another 30 min. The final suspension was filtered through a filter with a pore size of 0.45 µm. The PBCA nanoparticles were lyophilized for 24 h. A volume corresponding to a final concentration of 1% (m/v) of Tween 80 was added 30 min before release and cell culture testing.

Characterization of Poly(Butyl Cyanoacrylate) Nanoparticles

The physicochemical properties of PBCA nanoparticles, including parameters such as particle size, size distribution, and zeta potential, were evaluated through dynamic light scattering (DLS) using a LitesizerTM 500 (Anton Paar GmbH, Graz, Austria) equipped with a 658 nm single-frequency laser diode. Measurements were conducted in water at a detection angle of 175° in single-use cuvettes. The zeta potential was determined using electrophoretic light scattering in similar settings, employing omega cuvettes. All experiments were performed in triplicate. Nanoparticle tracking analysis (NTA) was employed to gain further insights into particle size and size distribution in the presence of release medium (PBS 7.4, 10% FBS). A Nanosight NS300 (Malvern Instruments, Malvern, UK) equipped with a 532 nm laser was utilized. During measurements, the chamber was maintained at a constant temperature. Data recording and analysis were conducted using NTA 3.2 (Dev Build 3.2.16, Malvern, UK) software. Each sample underwent three captures, each lasting 60 seconds, resulting in the detection of a minimum of 2000 valid particle tracks per sample. Particle diameters were calculated using the Stokes-Einstein equation and subsequently compared to reference measurements. For the determination of the total doxorubicin content in Cy5.5 labeled doxorubicin-loaded PBCA nanoparticles, spectrophotometric analysis was carried out (UV-1800, Shimadzu Corporation, Kyoto, Japan) at a wavelength of 481 nm after the dissolution of freeze-dried nanoparticles in DMSO. Spectrophotometric analysis at a wavelength of 480 nm was conducted to measure the concentration of free doxorubicin after the recovery of freeze-dried nanoparticles in water and subsequent separation of nanoparticles by ultracentrifugation (48,254 × g, 30 min, 5 °C) using an Avanti JXN-30 Centrifuge System (Beckman Coulter, Pasadena, CA, USA). The encapsulation efficiency of doxorubicin was determined as the percentage ratio of the difference between total and free doxorubicin to its total content in the sample.

Quantification of Doxorubicin Using High-Performance Liquid Chromatography

The analysis of the compound was conducted utilizing an HPLC system (Chromaster, VWR Hitachi, Tokyo, Japan) comprising a pump (5160), a fluorescence detector (5440), an autosampler (5260), and a column oven (5310). The stationary phase utilized in this study was a PerfectSil reversed-phase column (150 × 4.6 mm, pore size 110 Å, particle size 5 µm) obtained from Phenomenex Pte. Ltd., Singapore, coupled with a pre-column of the same material. The column was maintained at a constant temperature of 35 °C throughout the analysis. For the chromatographic separation, an isocratic method was employed with a flow rate of 1 mL/min. The mobile phase, consisting of acetonitrile and an aqueous solution of 0.1% trifluoroacetic acid, was mixed at a ratio of 32:68 (v/v). This composition of the mobile phase was crucial for achieving optimal separation and accurate detection of doxorubicin. Detection of the compound was accomplished using specific excitation and emission wavelengths set at 470 nm and 555 nm, respectively. These parameters were selected to ensure precise identification and quantification of the target compound. As presented in Figure S1, linearity was observed over a concentration range of 5–1000 ng/mL. The limit of detection and limit of quantification were determined to be 11.0 ng/mL and 33.2 ng/mL, respectively. Before injection, all samples were diluted with mobile phase.

In Vitro Drug Release Studies

Drug release studies were carried out utilizing a USP dissolution apparatus 2 sourced from Pharma Test Apparatebau AG (Hainburg, Germany). Each mini-vessel was equipped with a PTDR (Pharma Test Apparatebau AG, Hainburg, Germany).[25] A CE dialysis membrane with a molecular weight cutoff (MWCO) of 300 kDa was prepared according to the manufacturer's instructions and carefully mounted around the donor compartment as described previously.[30]

To estimate the in vivo release, the release medium was supplemented with 10% (v/v) fetal bovine serum (FBS) and 1% (v/v) PenStrep® solution to mimic physiological conditions.[30] PenStrep® was added to protect the release medium from microbiological contamination which could alter the release behavior over time. The experiments were conducted at a constant temperature of 37 °C ± 0.5 °C, and the stirring speed was precisely set to 50 revolutions per minute (rpm). To assess the degradation rate of doxorubicin, a quantity of 206 µg of the drug was introduced into the acceptor compartment. A total volume of 160 mL of the release medium was used for the experiments, which were performed over a duration of 6 hours. At predefined time intervals (5, 10, 15, 20, 30, 45, 60, 75, 90, 105 min, 2, 3, 4, 5, and 6 h), samples of 600 µL each were collected. After each sampling event, an equivalent volume of fresh release medium was added to the acceptor compartment to maintain a constant volume throughout the study.

Setting Up the Blood-Brain Barrier Transwell® System

Murine cerebral endothelial bEnd.3 cells (CRL-2299™; American Type Culture Collection) were maintained in DMEM cell culture medium supplemented with 10% FBS, 1% PenStrep®, and 1% Plasmocin®, and in tissue culture dishes at 37°C in a humidified incubator under a 5% CO_2 atmosphere. For treatment, bEnd.3 cells (passages 10–16) were seeded at a density of 3×10^5 cells on the Transwell® insert coated with 1% (v/v) collagen IV solution in PBS.

To evaluate the integrity of the BBB model, transendothelial electrical resistance (TEER) was measured on the Transwell® setup using a Millicell ERS-2 Voltohmmeter (Merck, Darmstadt, Germany) with a STX01 chopstick electrode.[31] The TEER of the insert without cells was measured and subtracted from the TEER obtained during the cell experiment yielding the net TEER values expressed as $\Omega \cdot cm^2$. All measurements were performed in triplicate.

Blood Cell Partitioning of PBCA Nanoparticles

To determine PBCA nanoparticles bound to the cellular fraction of the blood, 200 µL of PBCA nanoparticle suspension was incubated with 100 µL of mouse whole blood at 37 °C for 1 h. The suspension was subsequently centrifuged (800 rpm, 3 min, 25 °C) to separate the plasma and the cellular fraction of the blood. The two fractions were diluted with PBS to a volume of 500 µL, respectively, and fluorescence intensities of doxorubicin and Cy5.5 were measured with excitation at 470 and 566 nm and emission at 683 and 703 nm, respectively, using a Hidex Sense Beta microplate reader (Turku, Finland). Calibration curves for Cy5.5 and doxorubicin with the plasma and the RBCs were established, respectively (Figure S2). Briefly, the PBCA nanoparticle suspension was diluted to predetermined concentrations and the diluted suspensions (100 µL) were mixed with 100 µL of the plasma or RBCs at 37 °C for 1 h. The fluorescence of the mixtures was quantified after they were diluted to the volume of 500 µL with PBS.

Quantification of the Uptake of PBCA Nanoparticles by Immunocompetent Blood Cells

The in vivo uptake of the fluorescently labeled PBCA nanoparticles coated with polysorbate 80-coated by circulating immune cells was evaluated by flow cytometry. All animal studies were approved by local ethics committee of V. Serbsky Federal Medical Research Centre. BALB/c mice (female) were obtained from Andreevka Animal Center (Andreevka, Russia). The in vivo experiments were performed following the European Convention for the Protection of Vertebrate Animals, Directives 86/609/EEC, recommendations of the FELASE working group (1986, 86/609/EEC, ISSN 03780 6978), and the National Standard of the Russian Federation R 53434–2009 "Good Laboratory Practice". In brief, 200 µL of the PBCA nanoparticle suspension in 1% tween 80 (1 mg PBCA/mouse) was injected into the tail vein of the Balb/c mice (n = 6). The animals were anaesthetized by intraperitoneal injection of ketamine/xylazine 30 min after administration. The blood was collected through the cardiac puncture into heparin-containing syringes (100 U) and plasma was separated via centrifugation (800 ×g, 10 min, 23 °C). Gibco™ ACK Lysing Buffer was used for lysis of red blood cells (according to manufacturer's protocol). The cells were washed twice with FACS buffer (PBS, 2% BSA, 0.2% EDTA) and transferred to 96-well plates. The samples were incubated with anti-CD16/CD32 antibodies (for 10 min at +4 ◦C) to block non-specific Fc-mediated binding (1 µL per 1×10^6 cells). Then the samples were incubated with specific fluorescently labeled antibodies (30 min, 4 °C) to determine leukocyte subpopulations. The following antibody cocktails

were used: CD45 FITC leukocyte common antigen, and Ly6G BV and CD11b PE for neutrophils/monocytes, and CD4 Alexa Fluor 488 and B220 PE for lymphocytes. Alternatively, the antibody cocktail CD45 FITC, Ly6G BV, CD11b PE-Cy7 was used. The same antibodies with different fluorophores were chosen as an additional control for cell subpopulation detection using different laser lines.

The samples were analyzed on a FACS MoFlo XDP (Beckman Coulter, USA). The percent of different leukocyte subpopulations that capture nanoparticles (phagocytic cells) or are associated with the nanoparticles was determined as the percent of the nanoparticle-positive cells. Fluorophores, Brilliant Violet 421 (BV421; Ex/Em=408/422 nm), Fluorescein-5-isothiocyanate (FITC; Ex/Em=491/516 nm), Phycoerythrin (PE; Ex/Em=566/574 nm), Cyanine 5.5 (Cy5.5; Ex/Em=684/710 nm) were excited by 407, 488, 561 and 628 nm lasers, respectively Alexa Fluor 488 was excited by 488 laser, PE-Cyanine7 (PE-Cy7) dye was excited by 561 laser and detected using 780/60 filter set. The data were analyzed using Summit V5.2.0.7477 software. The representative samples were then fixed with 4% paraformaldehyde solution in PBS and transferred to a confocal microscope to determine the particle localization within the cells. Nikon confocal microscopy system Nikon A1R MP+ (Nikon Instruments, Japan) was used. The images were analyzed using NIS Elements AR software.

Transport Study of PBCA Nanoparticles in the BBB Model

Whole blood was collected from female C57BL/6 mice (aged 4–6 weeks) and mixed with ethylenediaminetetraacetic acid to a concentration of 10 μM. Ethics approval for this study was granted by the National University of Singapore (IACUC protocol number: R19-1195). The harvested blood was centrifuged at a speed of 800× g at ambient temperature for 3 min to remove the plasma and buffy coat by aspiration. Pellets containing the blood cells were resuspended in 1 mL of sterile PBS, before passing them through a Fisherbrand™ 40 μm Sterile Cell Strainer (Thermo Fisher Scientific, MA, USA). The filtrate was washed, centrifuged, and resuspended with 100 μL of plasma after aspiration of the PBS. For the preparation of nanoparticle-adhered cells, 2×10^6 of blood cells were incubated with 50 μL of the PBCA nanoparticle suspension (equivalent to 5.7 μg doxorubicin) in the absence or presence of 1% (v/v) Tweens 80 for 1 h at 37°C. A mixture of drug solution containing the same amount of doxorubicin and 2×10^6 blood cells were prepared as a control.

On day 5–7 after seeding cells when the TEER across cell monolayers measured was reaching a plateau, a transport study was initiated by the additions of various mixtures to the apical compartment as follows, a free drug solution with/without RBCs, a free drug containing Tween 80 with/without RBCs, a PBCA nanoparticle suspension with/without RBCs, and a PBCA nanoparticle suspension containing Tween 80 with/without RBCs. After incubation at 37 °C for 1 h, solution in the Transwell® basolateral compartment was collected for fluorescence measurement. Fluorescence measurements were conducted by quantifying the intensities of Cy5.5 and doxorubicin as mentioned above. All the tests were conducted in triplicate.

Statistical Analysis

Statistical analysis was performed utilizing GraphPad Prism 8 software, where a one-way ANOVA test was applied to identify significant differences ($p < 0.05$) among the experimental groups. Pharmacokinetic data was analyzed using Monolix 2020R1 (Lixoft, Antony, France) as described above.

Results and Discussion

Delivering anticancer drugs to the brain has been a major challenge in chemotherapy. Still, a variety of patients suffer from primary and secondary brain cancers with no access to effective treatments. PBCA nanoparticles are effective in animal models of glioblastoma multiforme. They were assumed to interact with the BBB and deliver high amounts of doxorubicin into the brain. In recent years, a very similar investigational drug product underwent Phase I clinical trials.[32] Here, we describe a so far undiscovered mechanism that explains their success. RBCs play a key role by facilitating nanoparticle-receptor interactions even hours after the delivery system disappears from the plasma. An advanced computer analysis together with relevant in vitro investigations outlines the importance of understanding brain drug delivery in more detail.

Computer Model Design

Initially, we modeled the pharmacokinetics of free doxorubicin reported for Doxil® and PBCA nanoparticles (refer to Figure 2A). Both studies included doxorubicin injections as reference formulations, as detailed by Siegal et al[24] and Gulyaev et al.[25] The stealth liposomes served as a control.

The rate constants for distribution into the brain (k_{B_in}, k_{B_out}), and periphery (k_{Peri_in}, k_{Peri_out}) as well as the elimination rate constants (k_{e_plasma}) were estimated.[24,25] PBCA nanoparticles were evaluated in healthy animals. Therefore, a tumor compartment (k_{T_in}, k_{T_out}) was modeled for Siegal et al (Doxil®) only (refer to Figure 2A).[24]

Afterward, a second computer model was designed which includes various formulation-related parameters of nanomedicines (refer to Figure 2B). The model design incorporates a nanocarrier compartment that characterizes the fraction of the drug delivery system circulating in the blood plasma (refer to Figure 2B, yellow section).

Upon release from the carrier (k_r), the distribution of the released drug is resembled by the structure of the first biodistribution model and utilizes the previously found rate constants (refer to Figure 2A). The parameter estimations will be presented in Biodistribution and Elimination of Free Doxorubicin. Doxorubicin is distributed into the periphery, the brain, and tumor compartments before it is eliminated from the body through hepatic or renal clearances.[32]

In addition to the release, the accumulation of nanomedicines, indicated by their half-life ($t_{1/2}$), signifies an alternative elimination pathway within the bloodstream. It can involve many organs such as the lungs or liver but may also involve interactions with blood cells.[25] Additional accumulation pathways enable direct targeting into the brain (k_{TargB}, $k_{CellTraf}$) and, regarding the liposomal delivery system Doxil®, the tumor area (k_{targT}). Brain targeting occurs through direct interactions (k_{targB}) which lead to a mass transfer from the blood plasma into the brain compartment. For PBCA nanoparticles, this mechanism did not explain pharmacokinetics in the brain sufficiently (refer to Figure S3). Hence, an additional delivery pathway ($k_{CellTraf}$) was included. The rationale for hypothesizing a drug delivery pathway through cellular shuttling will be further introduced in Biodistribution and Elimination of Nanomedicines.

Biodistribution and Elimination of Free Doxorubicin

To model the biodistribution of free doxorubicin, an injection of the absolute dose into the central compartment of the first biodistribution model (refer to Figure 2A) was assumed. Gulyaev et al[25] reported the concentration-time profiles

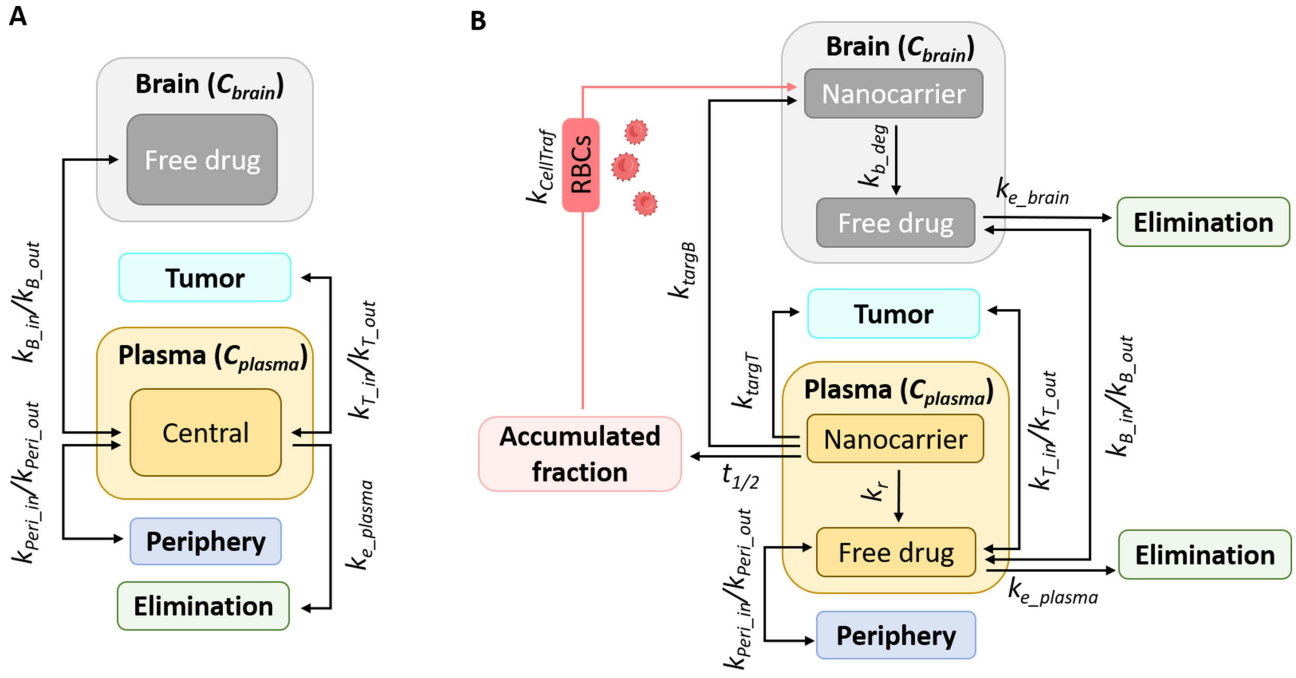

Figure 2 Illustration of the biodistribution model simulating the indirect and direct pathways into the brain. (**A**) The biodistribution after administration of doxorubicin solution. (**B**) The biodistribution after administration of doxorubicin nanocarriers.

found in the plasma and brain, in healthy Wistar rats at a dose of 5 mg·kg^{-1}.[25] As compared to common cancer models, the BBB of healthy animals is fully intact. Under these conditions, the doxorubicin concentration in the brain remained below the detection limit (100 ng•g^{-1}). Overlays of the simulated and observed plasma and brain concentrations are presented in Figure 3A and B). The model predictions exhibit strong agreement with the observed concentrations and demonstrate an exceptional representation of the in vivo data, as indicated by the goodness-of-fit plots (Figure S4A–D), which highlight the low prediction error.

The population parameters obtained from this study were employed to characterize the dynamics of the free drug and facilitate a model-based deconvolution of the pharmacokinetics of PBCA nanoparticles.

A similar model prediction was carried out for pharmacokinetic data reported by Siegal et al[24] This investigation involved a 6 mg·kg^{-1} injection of an aqueous doxorubicin solution into female Fisher rats bearing methylcholantrene-induced histiocytoma.[24] The tumor potentially leads to a disruption of the BBB. Plasma, brain, and tumor concentrations of doxorubicin were reported.[24] The overlays of the predicted versus the observed plasma, brain, and tumor concentrations are presented in Figure 3C–E. The diffusion of doxorubicin was well-described, as indicated by the goodness-of-fit plots (Figure S4E–J). All model parameters have been summarized in Table 1.

Biodistribution and Elimination of Nanomedicines

Following the injection, nanomedicines persist within the vascular system, resulting in increased plasma concentrations. This heightened presence in the bloodstream can facilitate enhanced diffusion into diverse organs, including the brain. Therefore, accurate quantification of the amounts delivered through nanocarrier-mediated delivery necessitates the consideration of population parameters of free doxorubicin in the brain and the plasma. Both are accessible through a model-based deconvolution resulting in the release (k_r) and brain diffusion rate constants (k_{B_in}, k_{B_out}) (Table 1).

As a next step, the accumulation ($t_{1/2}$) and targeting rate constants (k_{TargB} *and* k_{TargT}) of each drug delivery system were identified. Doxil® consists of pegylated stealth liposomes that exhibit minimal interactions with blood cells.[33]

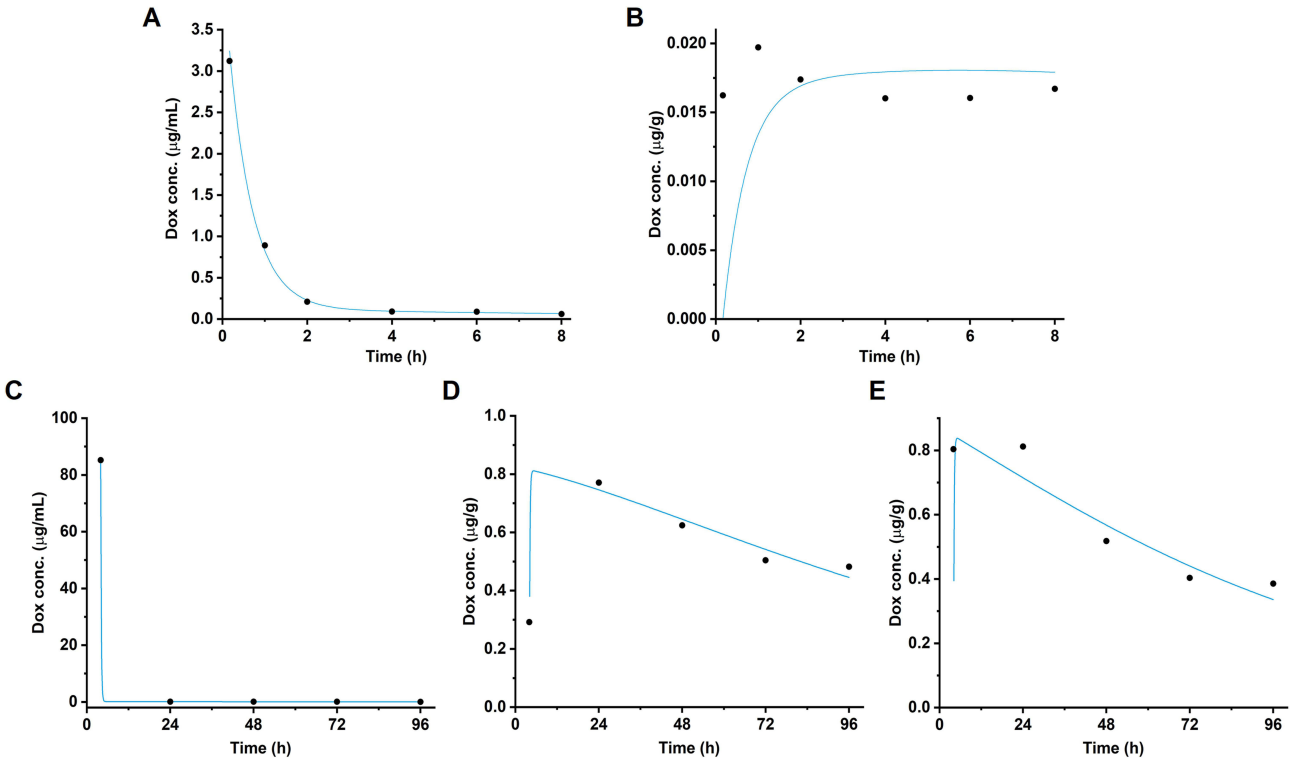

Figure 3 Observed and simulated doxorubicin concentration-time profiles following intravenous administration of free doxorubicin. Overlay between the predicted and the observed concentrations in (**A**) plasma and (**B**) brain observed by Gulyave et al[25] and in (**C**) plasma, (**D**) brain, and (**E**) tumor observed by Siegal et al.[24]

Table 1 Parameter Estimation for Pharmacokinetic Behavior Following Administration of Free Doxorubicin

Parameter	Doxorubicin Solution (5 mg•kg^{-1})	Doxorubicin Solution (6 mg•kg^{-1})
Body weight (g)	190	190
f_{brain} (%)	1.240	1.104
Tumor weight (g)	–	0.02
k_{Peri_in} (h^{-1})	0.73	1.98
k_{Peri_out} (h^{-1})	0.16	0.025
k_{B_in} (h^{-1})	3.8×10^{-5}	4.9×10^{-4}
k_{B_out} (h^{-1})	0.035	0.012
k_{e_plasma} (h^{-1})	0.96	4.12
k_{T_in} (h^{-1})	–	0.9×10^{-4}
k_{T_out} (h^{-1})	–	0.016
V_{plasma} (mL)	295.09	13.38

The mode of accumulation has been described in the previous literature and is mainly due to the extravasation of liposomes in the tumor area.[24] Our model-based analysis confirmed this delivery pathway. The model predictions as well as the observed doxorubicin levels in plasma, brain, and tumor are presented in Figure 4. They were in good alignment as indicated by the diagnostic plots (refer to Figure S5), and outlined a direct interaction between the circulating fraction (determined in the blood plasma) and the BBB (k_{TargB}). Consequently, the increase in brain concentrations corresponded to a decrease in the plasma concentration.

The resulting population parameters are presented in Table 2. A long half-life of more than 40 h as well as a slow release rate (3.5×10^{-6} h^{-1}) have been identified.

Expectedly, targeted delivery into the brain (k_{targB}) remained at a low level (5.9×10^{-5} h^{-1}) while the tumor-targeting rate (k_{targT}, 2×10^{-4} h^{-1}) was significantly higher. The enhanced permeability and retention effect enables the liposomes to penetrate the tumor tissue but does not provide access to the rest of the brain.

A similar model structure was used to predict the biodistribution of PBCA nanoparticles. The respective study was conducted on healthy animals. Accordingly, the model design did not include a tumor compartment. However, while the plasma concentrations were sufficiently described by the model structure, there was a misalignment between plasma and brain pharmacokinetics. After the injection, PBCA nanoparticles were rapidly eliminated from the blood plasma, and the increase in the brain concentrations was observed with considerable delay. This lag time could not be explained by a direct interaction between the circulating particle fraction and the BBB.

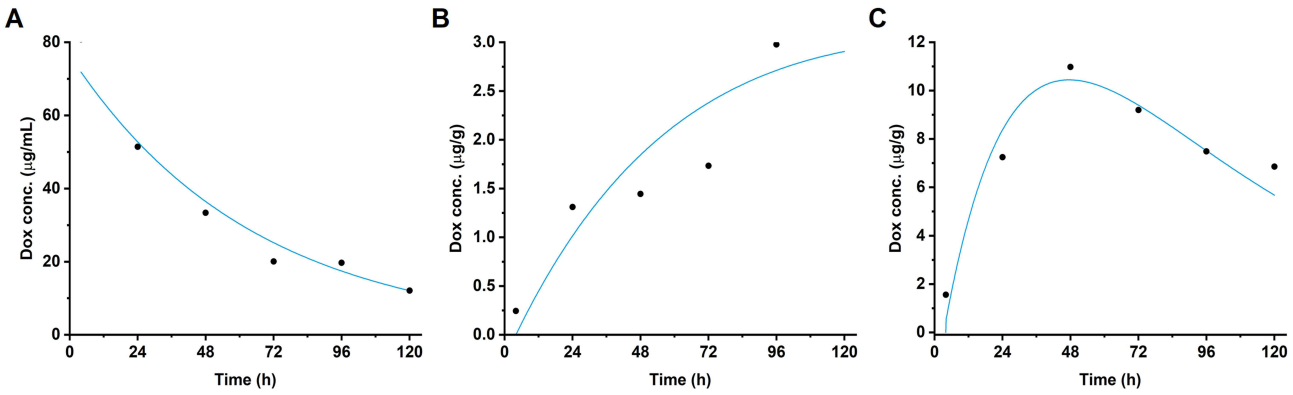

Figure 4 Observed and simulated doxorubicin concentration-time profiles following intravenous administration of Doxil®. Overlay between the predicted and the observed concentrations in (**A**) plasma, (**B**) brain, and (**C**) tumor for the pharmacokinetics observed by Siegal et al.[24]

Table 2 Parameter Estimation for Pharmacokinetic Behavior Following Administration of Doxil®[24] and PBCA Nanoparticles[25]

Parameter	Doxil® (Stealth Liposome) (6 mg•kg^{-1})	PBCA Nanoparticle with Tween 80 (5 mg•kg^{-1})
k_{targB} (h^{-1})	5.9 × 10^{-5}	1.4 × 10^{-7}
k_{targT} (h^{-1})	2.0 × 10^{-4}	–
k_{b_deg} (h^{-1})	2.9 × 10^{-5}	4.17
$k_{CellTraf}$ (h^{-1})	–	0.32
k_r (h^{-1})	3.5 × 10^{-6}	1.03
$t_{1/2}$ (h)	40.12	4.57
k_{e_brain} (h^{-1})	0.32	1.24

Gulyaev et al attributed the cascade of events to the time-consuming process of endocytosis.[25] However, the quantification of doxorubicin concentrations from brain homogenate would account for the drug bound in these cellular pathways, prompting us to seek an alternative explanation.

Recent literature describes a hitchhiking mechanism whereby polymer nanoparticles adsorb to the surface of red blood cells (RBCs) from where they are distributed into multiple organs.[33] This aligns with the short plasma half-life of PBCA nanoparticles and would further enable the accumulated fraction to be involved in brain delivery.

Considering this potential interaction between PBCA nanoparticles and blood cells,[34] we introduced the respective cellular shuttling mechanism ($k_{CellTraf}$) to the model design (refer to Figure 2B). The new model structure was in good alignment with the data reported by Gulyaev et al[25] as outlined in Figure 5. The quality of the simulation is further confirmed by the diagnostic plots (Figure S5).

Direct interactions between the circulating fraction of PBCA nanoparticles and BBB remained at a very low level (1.4 × 10^{-7} h^{-1}). Hence, the cell shuttling mechanism was the more efficient delivery pathway (0.32 h^{-1}). As compared to Doxil® which delivers doxorubicin mainly through extravasation, a more than 1000-fold increase in the total transport rate (2.59 × 10^{-4} vs 0.32 h^{-1}) has been observed. To comprehensively understand the observed differences in vivo, it is imperative to examine multiple factors. The surface pegylation of Doxil®, a liposomal delivery system, plays a key role in reducing cellular interactions,[24] including those with vascular endothelial cells. This process inhibits interactions with receptors on the surface of the BBB. The efficiency of brain uptake is significantly influenced by the likelihood of

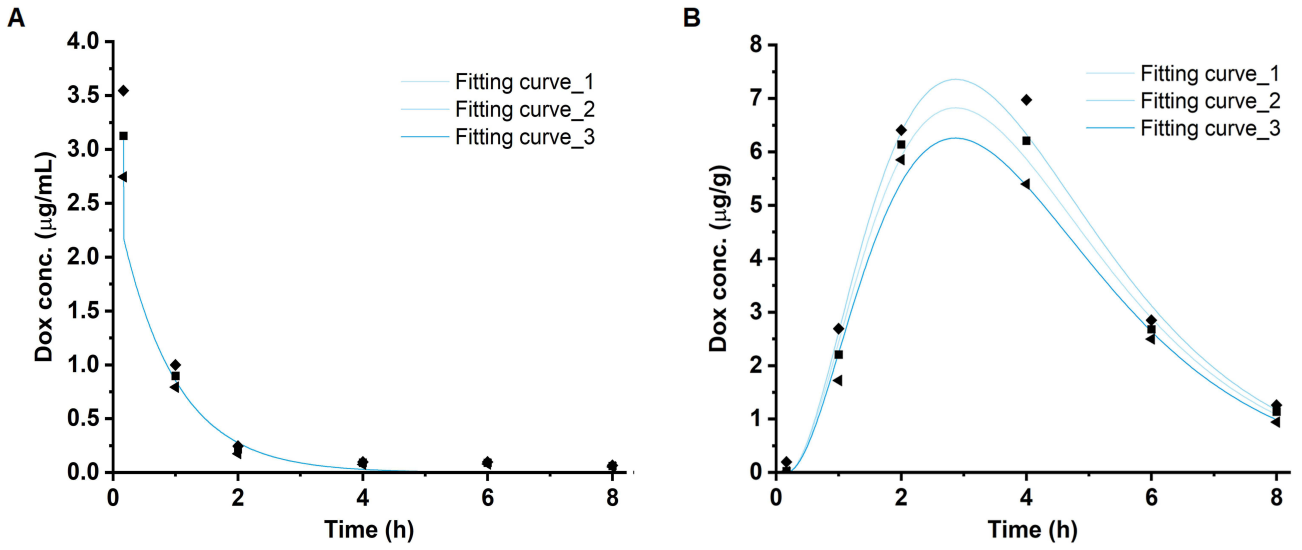

Figure 5 Observed and simulated doxorubicin concentration-time profiles following intravenous administration of PBCA nanoparticles. Overlay between the predicted and the observed concentrations in (**A**) plasma and (**B**) brain for the pharmacokinetics observed by Gulyaev et al.[25] The observed upper (◆), mean (■) and lower (◀) values were fitted, respectively. An overlay using the model structure without an indirect (cell-mediated) accumulation pathway was unsuccessful and is presented in the Figure S3).

extravasation within tumor regions in the brain, which represent a minor fraction of the vascular system. Conversely, PBCA nanoparticles are actively targeted and internalized into the brain by receptors. Despite their relatively brief presence in blood plasma, their interaction with blood cells likely results in an extended exposure period. Additionally, the role of efflux transporters, which actively pump doxorubicin back into the bloodstream, must be considered.[18,35] Existing literature suggests that nanoparticles can bypass these efflux mechanisms which further increases the uptake through the cell-mediated pathway.[22,23,36]

While many investigations have focused on the cell interactions of Doxil®, little is known about the blood interactions of PBCA nanoparticles. Consequently, our next investigations were focused on collecting further evidence for the presence of this brain delivery superhighway.

In Vitro Studies with PBCA Nanoparticles

To confirm our hypothesis, we defined three key objectives. Firstly, we needed to quantify the release kinetics of PBCA nanoparticles. The release is a competing process that reduces the availability of doxorubicin involved in particle-based delivery. Secondly, we conducted a blood partitioning study which provides more information on the extent of the association between PBCA nanoparticles and blood cells. Thirdly, we investigated the ability of the nanoparticles to interact with receptors at the surface of the BBB in the presence of blood cells.

Characteristics of PBCA Nanoparticles

As a first step, we synthesized PBCA nanoparticles following the protocol described in the literature.[25] The polymer was labeled with the fluorescent dye Cy5.5 for in vitro tracking of the delivery system.

A hydrodynamic diameter of 206.3 ± 12.1 nm (PDI: 0.073 ± 0.052) was achieved on average. The unloaded particles were comparable in size but exhibited a slightly lower (more negative) zeta potential (Table 3). NTA measurements revealed a smaller diameter of approximately 100 nm with a narrow size distribution (refer to Figure S6A). It is worth noting that a misalignment in particle sizes measured by these two methods has been frequently reported. While DLS often captures the presence of larger agglomerates, the size distribution measured for particles in the nanoscale is much more resolved using the NTA.

Furthermore, the morphology of the delivery system was analyzed using scanning electron microscopy and revealed an almost perfectly spherical shape as well as a size distribution in the expected range (refer to Figure S6B). Upon storage, the aqueous suspension was stable for 2 years without significant changes in hydrodynamic diameter or PDI (ANOVA).

Afterward, the in vitro release behavior of these nanoparticles was tested using the dispersion releaser technology.[30] Model-based deconvolution of the in vivo data (reported by Gulyaev et al)[25] indicated a rapid release (1.03 h^{-1}). The outcome of the in vitro study is presented in Figure 6. Approximately 78% of doxorubicin was released within 3 h in a biorelevant release medium.

The observed release kinetics deviated from the model predictions, as illustrated in Figure 6 (inset). Notably, the in vitro release, which conformed to a first-order diffusion model (Figure 6, inset – represented by the grey dashed line), achieved approximately 40% of the in vivo release rate (Figure 6, inset – depicted as a black solid line).

The dispersion releaser, designed for biopredictive evaluation of particle formulations, demonstrated a noteworthy correlation with the in vivo release performances, as reported in previous studies.[26,29] These correlations were established across a wide range of formulations using preclinical and clinical pharmacokinetic data.[12,29,30] Still, the assay does

Table 3 Physicochemical Parameters of Doxorubicin-Loaded and Unloaded PBCA Nanoparticles Labeled with Cy5.5

Size Distribution		Zeta Potential (mV)	EE%	Loading Capacity (μg per mg polymer)
Particle Diameter (nm)	PDI			
206.3 ± 12.1	0.073 ± 0.052	−2.6 ± 1.1	35.8 ± 4.1	6.2 ± 0.3
203.9 ± 0.7 nm	0.150 ± 0.012	−10.2 ± 0.1 mV		

Note: Data are presented as mean ± standard deviation (n = 3).
Abbreviations: EE, encapsulation efficiency; PDI, polydispersity index.

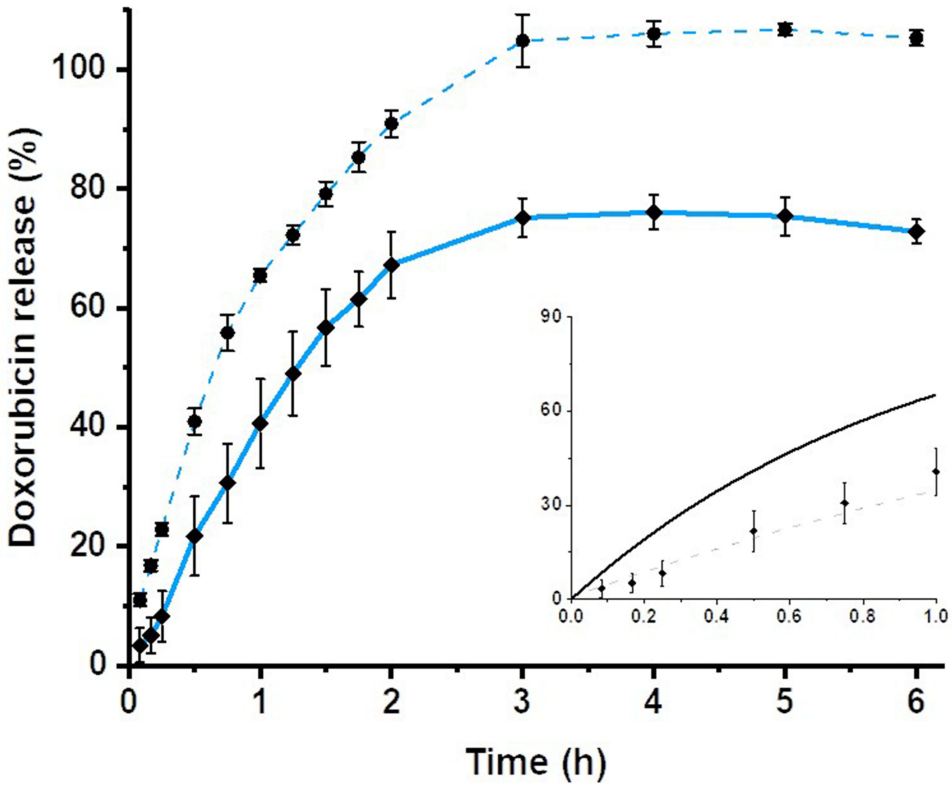

Figure 6 Doxorubicin permeation (dashed blue line, black circles) and release from the PBCA nanoparticles (solid blue line, black diamonds) over 6 h (n = 3). The inset compares in vitro (black diamonds fitted with a first-order diffusion model indicated by the grey dashed line) with the in vivo release rate determined by the in silico model (black line).

resemble the in vivo environment completely. Notably, the shear rate is considerably higher in this setup compared to the in vivo conditions, and there is a discernible delay in the appearance of the released drug in the acceptor compartment, primarily attributed to the influence of the dialysis rate.

Despite the elevated shear rate, more than 20% of the total dose of doxorubicin remained embedded in the particle matrix. The brain concentrations show a considerable increase approximately 1–2 hours after injection (refer to Figure 5B). Therefore, our findings provided a robust foundation for further investigations of the cell-mediated drug delivery pathway. The fraction of the drug remaining within the particles could reasonably account for the enhanced brain transport, taking into consideration that the brain comprises merely 2% of the total body mass.[8]

Interaction of PBCA Nanoparticles with Blood Cells

Initially, the formulation was incubated with whole blood to investigate the partitioning of doxorubicin and PBCA between the plasma and blood cells, aiming to establish its connection to the observed brain delivery process. The preparations did not induce hemolysis for at least 1 h.

As presented in Table 4, approximately 35% of doxorubicin was bound to the blood cells while a significant fraction (65%) remained in the plasma. Considering the fast release of doxorubicin from the nanoparticles, we further quantified

Table 4 Average Values of Free and Blood Cell-Bound Doxorubicin and PBCA Nanoparticle Fractions

	Doxorubicin		PBCA Nanoparticle	
	Plasma	Blood Cells	Plasma	Blood Cells
Bound fraction %	65	35	10	90

Note: Data are presented as mean ± standard deviation (n = 3).

the distribution of PBCA nanoparticles by determining the Cy5.5 signal. Our findings indicate that 90% of the nanoparticles were indeed attached to blood cells.

Given the substantial release, we hypothesized an unspecific interaction with the cellular surface. Active uptake would potentially inhibit the doxorubicin release into the plasma. Still, we wanted to understand the interaction in more detail.

Circulating immune cells are known to interact with nanoparticles. To explore their involvement, mice were intravenously injected with the formulation, and blood samples were collected 30 minutes after administration. The flow cytometry indicates that the nanoparticles were efficiently captured by immune cells expressing the CD11b marker (most probably monocytes or neutrophils). The strongest association was observed for double-positive (CD11b+, Ly6G+) cells (neutrophils) of which approximately 60% tested positive for the nanoparticles (Figure 7A).

Confocal microscopy imaging (Figures 7B and C) confirmed the effective capture of PBCA-Cy5.5 nanoparticles by leukocytes. These findings align with previous studies where nanoparticles larger than 200 nm in diameter were observed to exhibit a strong association with neutrophils.[7,37]

Nanoparticle interactions with B cells appear to be infrequent, as their association with the nanoparticles was approximately 10% (Figure 7A) and not observed in the confocal microscopy samples. Figure 7C demonstrates the capture of nanoparticles by CD45+ cells, while their association with B220-expressing cells was not detected.

In Vitro BBB Assay

As a next step, we explored BBB interactions in more detail. For this in vitro experiment, we utilized bEnd.3 cells, a murine endothelial cell line that forms tight junctions and can be used to replicate the endothelial barrier of the BBB (Figure 8A). The formation of a continuous monolayer was monitored using transendothelial electrical resistance (TEER) measurements.

As presented in Figure 8B, the TEER plateaued at the level of 124 $\Omega \cdot cm^2$, 48 h after cell seeding on the collagen IV coated membranes which indicated the formation of tight junctions. The experiment was initiated 96 hours after seeding.

Initially, the TEER decreased to approximately 100 $\Omega \cdot cm^2$ including the control groups without doxorubicin and PBCA nanoparticles, indicating stress due to a change in the medium composition. After 24 h of treatment, the stable TEER suggested that the bEnd.3 monolayer was still intact and neither of the samples led to a disruption of the cellular barrier.

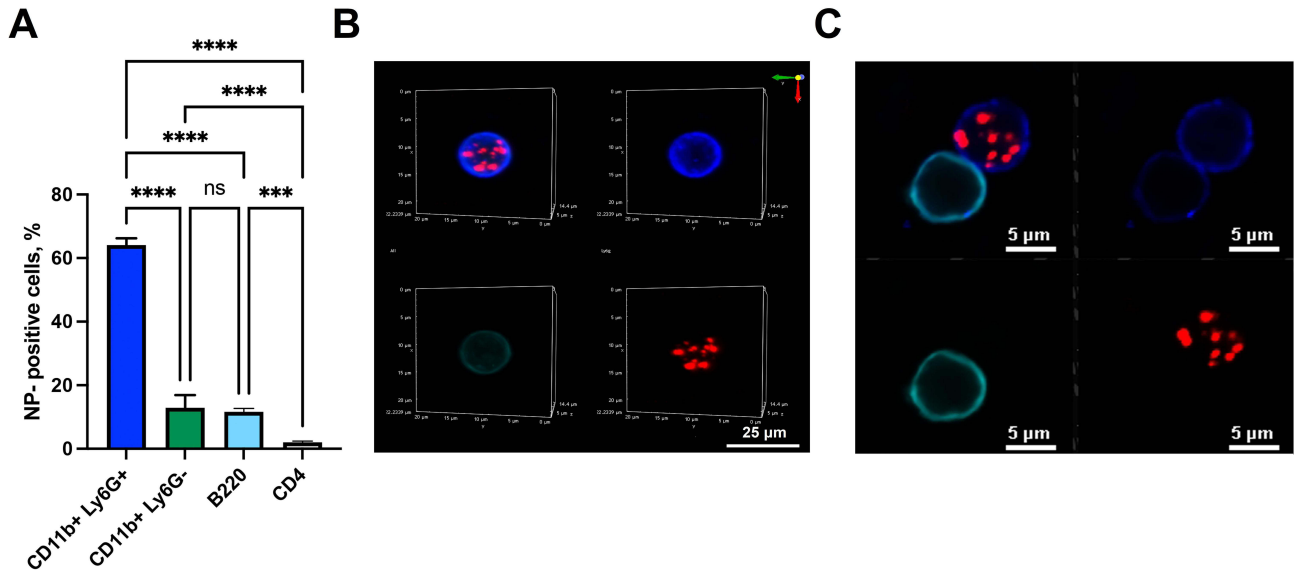

Figure 7 Evaluation of PBCA-Cy5.5 nanoparticle uptake by circulating immune cells. (**A**) The percentage of immune cells bound by PBCA nanoparticles measured by flow cytometry. The data are represented as percent of the NP-positive cells (mean ± SD, $n = 6$; ****$p < 0.0001$; ***$p < 0.001$; ns: non-significant). (**B**) Visualization of PBCA-Cy5.5 nanoparticles coated with polysorbate 80 (red) capture by CD11b PE (green), Ly6G BV (blue) positive cell (neutrophil). (**C**) Visualization of PBCA-Cy5.5 nanoparticles coated with polysorbate 80 (red) interaction with lymphocytes. CD45 FITC (blue), B220 PE (green).

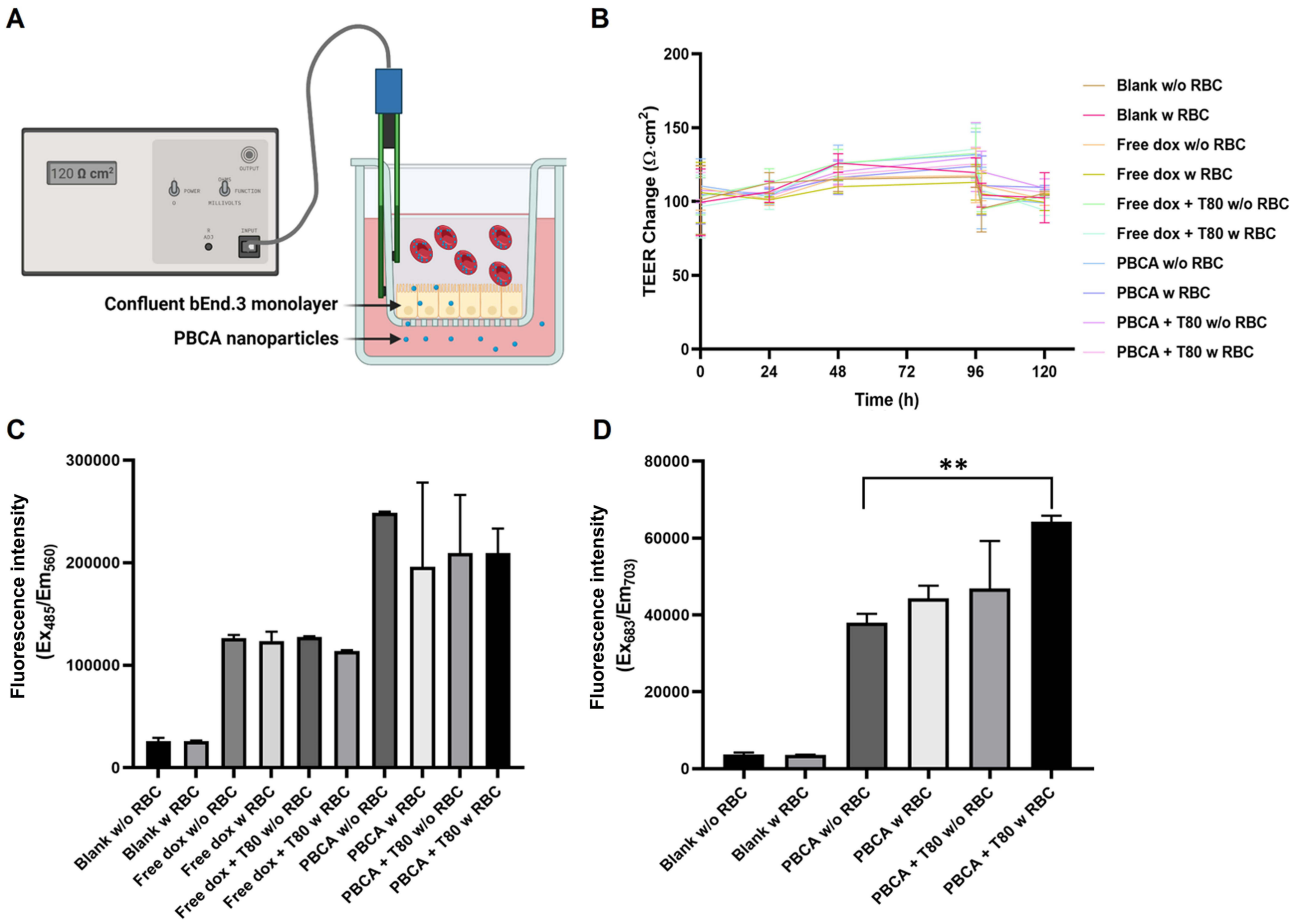

Figure 8 Transport of PBCA nanoparticles across the blood-brain barrier model. (**A**) Transwell® setup with an apical compartment seeded with bEnd.3 cell monolayers and a basolateral compartment. The chopstick electrode measured TEER across the membrane determining the confluency of the bEnd.3 monolayer. Media from the basolateral compartment were collected for fluorescence measurement 1 h after adding test solutions. (**B**) Mean TEER values of bEnd.3 monolayer incubating with different test solutions over 120 h (n = 3). Mean (**C**) doxorubicin and (**D**) Cy5.5 fluorescence intensity in the basolateral compartment (n = 3). The linearity of the fluorescence detection method was confirmed and is presented in Figure S5 (**p < 0.05).

In Figure 8C, the detection of the doxorubicin signal in the basolateral compartment after 24 hours of incubation is illustrated. The presence of PBCA nanoparticles significantly enhanced the transport of doxorubicin (p = 0.0014) across the BBB model compared to the free drug. Neither Tween 80 nor the blood cells affected the transport of free doxorubicin across the bEnd.3 monolayer. Furthermore, there was no significant difference (p = 0.64) observed between the PBCA nanoparticle groups with or without blood cells. It should be noted that the rapid release characteristics of PBCA nanoparticles may lead to an overestimation of nanoparticle-related transport. To track the nanoparticles, we measured the Cy5.5 fluorescence signal of the carrier.

Previous literature investigated the mechanism underlying the enhanced uptake of the nanoparticles into the brain without considering the potential involvement of blood cells.[4,38] Before administration, the nanoparticles are coated with polysorbate 80 which attracts apolipoproteins from the blood plasma. They are responsible for interactions with various receptors at the surface of the BBB.[4] As illustrated in Figure 8D, the highest uptake was observed in the group treated with blood cell-preincubated Tween 80-coated PBCA nanoparticles. This suggests that a combination of blood cell hitchhiking and particle coating enhances the permeation of PBCA nanoparticles across the endothelial cell monolayer. Notably, the presence of Tween 80 or RBCs alone did not yield significant increases in transport. In this context, the limitations of the in vitro set-up must be considered. Neither the limited volume of the experiment nor the negligible shear forces promote the dissociation of apolipoproteins from the carrier. Additionally, a high amount of free doxorubicin

provides a non-physiological concentration gradient that potentially allows more doxorubicin to pass through the artificial BBB.

Conclusion

In conclusion, the rising popularity of data mining and computational learning strategies in contemporary literature has led us to a remarkable discovery. Our in-depth analysis of biodistribution studies dating back two decades has expanded our understanding beyond the established concepts related to the prolonged vascular circulation of drugs and nanoparticles adhering to blood cell surfaces, and its effects on in vivo distribution patterns.

Our findings firmly establish that these hitchhikers actively participate in receptor-mediated uptake, with a particular focus on how PBCA nanoparticles efficiently target the brain through cellular hitchhiking, thereby facilitating and enhancing their delivery to the CNS. As a point of comparison, we investigated the brain distribution of Doxil®, a formulation of stealth liposomes engineered to minimize cellular interactions and adhere to expected distribution patterns. While Doxil® undeniably improves plasma pharmacokinetics, its reduced cellular interactions significantly hinder uptake into the brain through the cellular hitchhiking pathway.

Our study presents compelling evidence confirming the existence and effectiveness of the cell-mediated delivery pathway for transporting drugs across the blood-brain barrier. Furthermore, our findings emphasize the paramount importance of employing refined data analysis methods to advance the field of nanomedicine.

Declaration of Generative AI in Scientific Writing

During the preparation of this work, the authors used the AI tool ChatGPT v3.5 to improve the language and flow of speech. After using this tool/service, the authors reviewed and edited the content as needed and take full responsibility for the content of the publication.

Dedication

This work is dedicated to the cherished memory of Dr. David Begley, Senior Lecturer at King's College London, whose profound impact on our understanding of brain delivery superhighways will forever be remembered.

Acknowledgment

The authors acknowledge Lixoft (Antony, France) for an academic license of Monolix Suite 2020R. M.G. W. acknowledges the National University of Singapore, Faculty of Science, and the Ministry of Education (Startup grant no. A-0004627-00-00 and Tier 1 grant no. A-0004337-00-00) for financial support. Cell studies were carried out within the state assignment of Ministry of Science and Higher Education of the Russian Federation (project FSSM-2022-0003). The graphical abstract was created with the AI tool ChatGPT v4 (DALL-E).

Author Contributions

All authors made a significant contribution to the work reported, whether that is in the conception, study design, execution, acquisition of data, analysis and interpretation, or in all these areas; took part in drafting, revising or critically reviewing the article; gave final approval of the version to be published; have agreed on the journal to which the article has been submitted; and agree to be accountable for all aspects of the work.

Disclosure

The authors report no conflicts of interest in this work.

References

1. Cheo STT, Lim GH, Lim KHC. Glioblastoma multiforme outcomes of 107 patients treated in two Singapore institutions. *Singapore Med J*. 2017;58(1):41–45. doi:10.11622/smedj.2016044
2. Liang SK, Hsieh MS, Lee MR, Keng LT, Ko JC, Shih JY. Real-world experience of Afatinib as a first-line therapy for advanced EGFR mutation-positive lung adenocarcinoma. *Oncotarget*. 2017;8(52):90430–90443. doi:10.18632/oncotarget.19563

3. Lombardo SM, Schneider M, Türeli AE, Günday Türeli N. Key for crossing the BBB with nanoparticles: the rational design. *Beilstein J. Nanotechnol*. 2020;11:866–883. doi:10.3762/bjnano.11.72
4. Wohlfart S, Gelperina S, Kreuter J. Transport of drugs across the blood-brain barrier by nanoparticles. *J Control Release*. 2012;161(2):264–273. doi:10.1016/j.jconrel.2011.08.017
5. Zhao M, van Straten D, Broekman MLD, Preat V, Schiffelers RM. Nanocarrier-based drug combination therapy for glioblastoma. *Theranostics*. 2020;10(3):1355–1372. doi:10.7150/thno.38147
6. Feczko T, Piiper A, Ansar S, et al. Stimulating brain recovery after stroke using theranostic albumin nanocarriers loaded with nerve growth factor in combination therapy. *J Control Release*. 2019;293:63–72. doi:10.1016/j.jconrel.2018.11.017
7. Ulbrich K, Hekmatara T, Herbert E, Kreuter J. Transferrin- and transferrin-receptor-antibody-modified nanoparticles enable drug delivery across the blood–brain barrier (BBB). *Eur J Pharm Biopharm*. 2009;71(2):251–256. doi:10.1016/j.ejpb.2008.08.021
8. Zensi A, Begley D, Pontikis C, et al. Human serum albumin nanoparticles modified with apolipoprotein A-I cross the blood-brain barrier and enter the rodent brain. *J Drug Target*. 2010;18(10):842–848. doi:10.3109/1061186X.2010.513712
9. Zensi A, Begley D, Pontikis C, et al. Albumin nanoparticles targeted with Apo E enter the CNS by transcytosis and are delivered to neurones. *J Control Release*. 2009;137(1):78–86. doi:10.1016/j.jconrel.2009.03.002
10. Gosselet F, Loiola RA, Roig A, Rosell A, Culot M. Central nervous system delivery of molecules across the blood-brain barrier. *Neurochem Int*. 2021;144:104952. doi:10.1016/j.neuint.2020.104952
11. Kovshova T, Osipova N, Alekseeva A, et al. Exploring the interplay between drug release and targeting of lipid-like polymer nanoparticles loaded with doxorubicin. *Molecules*. 2021;26(4):831. doi:10.3390/molecules26040831
12. Pardridge WM, Chou T. Mathematical models of blood-brain barrier transport of monoclonal antibodies targeting the transferrin receptor and the insulin receptor. *Pharmaceuticals*. 2021;14(6):535. doi:10.3390/ph14060535
13. Pardridge WM. Delivery of biologics across the blood-brain barrier with molecular trojan horse technology. *BioDrugs*. 2017;31(6):503–519. doi:10.1007/s40259-017-0248-z
14. Kouhi A, Pachipulusu V, Kapenstein T, Hu P, Epstein AL, Khawli LA. Brain disposition of antibody-based therapeutics: dogma, approaches and perspectives. *Int J Mol Sci*. 2021;22(12):6442. doi:10.3390/ijms22126442
15. Pulgar VM, Berlin S, Olszakier S, Pahari SK, Kahn I. Transcytosis to cross the blood brain barrier, new advancements and challenges. *Front Neurosci*. 2019;13:12. doi:10.3389/fnins.2019.00012
16. Sade H, Baumgartner C, Hugenmatter A, Moessner E, Freskgård P-O, Niewoehner J. A Human blood-brain barrier transcytosis assay reveals antibody transcytosis influenced by pH-dependent receptor binding. *PLoS One*. 2014;9(4):e96340. doi:10.1371/journal.pone.0096340
17. Bronger H, König J, Kopplow K, et al. ABCC drug efflux pumps and organic anion uptake transporters in human gliomas and the blood-tumor barrier. *Cancer Res*. 2005;65(24):11419–11428. doi:10.1158/0008-5472.CAN-05-1271
18. Parvez MM, Sadighi A, Ahn Y, Keller SF, Enoru JO. Uptake transporters at the blood-brain barrier and their role in brain drug disposition. *Pharmaceutics*. 2023;15(10):2473. doi:10.3390/pharmaceutics15102473
19. Barui S, Saha S, Mondal G, Haseena S, Chaudhuri A. Simultaneous delivery of doxorubicin and curcumin encapsulated in liposomes of pegylated RGDK-lipopeptide to tumor vasculature. *Biomaterials*. 2014;35(5):1643–1656. doi:10.1016/j.biomaterials.2013.10.074
20. Hoosain FG, Choonara YE, Tomar LK, et al. Bypassing P-glycoprotein drug efflux mechanisms: possible applications in pharmacoresistant schizophrenia therapy. *Biomed Res Int*. 2015;2015:484963. doi:10.1155/2015/484963
21. Alyautdin RN, Petrov VE, Langer K, Berthold A, Kharkevich DA, Kreuter J. Delivery of loperamide across the blood-brain barrier with polysorbate 80-coated polybutylcyanoacrylate nanoparticles. *Pharm Res*. 1997;14(3):325–328. doi:10.1023/A:1012098005098
22. Wohlfart S, Khalansky AS, Gelperina S, Begley D, Kreuter J. Kinetics of transport of doxorubicin bound to nanoparticles across the blood-brain barrier. *J Control Release*. 2011;154(1):103–107. doi:10.1016/j.jconrel.2011.05.010
23. Kreuter J, Ramge P, Petrov V, et al. Direct evidence that polysorbate-80-coated poly(butylcyanoacrylate) nanoparticles deliver drugs to the CNS via specific mechanisms requiring prior binding of drug to the nanoparticles. *Pharm Res*. 2003;20(3):409–416. doi:10.1023/A:1022604120952
24. Gulyaev AE, Gelperina SE, Skidan IN, Antropov AS, Kivman GY, Kreuter J. Significant transport of doxorubicin into the brain with polysorbate 80-Coated nanoparticles. *Pharm Res*. 1999;16(10):1564–1569. doi:10.1023/A:1018983904537
25. Janas C, Mast MP, Kirsamer L, et al. The dispersion releaser technology is an effective method for testing drug release from nanosized drug carriers. *Eur J Pharm Biopharm*. 2017;115:73–83. doi:10.1016/j.ejpb.2017.02.006
26. Modh H, Fang DJ, Ou YH, et al. Injectable drug delivery systems of doxorubicin revisited: in vitro-in vivo relationships using human clinical data. *Int J Pharm*. 2021;608:121073. doi:10.1016/j.ijpharm.2021.121073
27. Li Z, Ramirez G, Tang R, et al. Modeling digestion, absorption, and ketogenesis after administration of tricaprilin formulations to humans. *Eur J Pharm Biopharm*. 2023;182:41–52. doi:10.1016/j.ejpb.2022.11.022
28. Nagpal S, Braner S, Modh H, et al. A physiologically-based nanocarrier biopharmaceutics model to reverse-engineer the in vivo drug release. *Eur J Pharm Biopharm*. 2020;153:257–272. doi:10.1016/j.ejpb.2020.06.004
29. Mast MP, Modh H, Champanhac C, et al. Nanomedicine at the crossroads - a quick guide for ivivc. *Adv Drug Deliv Rev*. 2021;179:113829. doi:10.1016/j.addr.2021.113829
30. Traynard P, Ayral G, Twarogowska M, Chauvin J. Efficient pharmacokinetic modeling workflow with the monolixsuite: a case study of remifentanil. *CPT Pharmacometrics Syst Pharmacol*. 2020;9(4):198–210. doi:10.1002/psp4.12500
31. Ruiz-Molina D, Mao X, Alfonso-Triguero P, et al. Advances in preclinical/clinical glioblastoma treatment: can nanoparticles be of help? *Cancer*. 2022;14(19):4960. doi:10.3390/cancers14194960
32. Pippa LF, Oliveira ML, Rocha A, de Andrade JM, Lanchote VL. Total, renal and hepatic clearances of doxorubicin and formation clearance of doxorubicinol in patients with breast cancer: estimation of doxorubicin hepatic extraction ratio. *J Pharm Biomed Anal*. 2020;185:113231. doi:10.1016/j.jpba.2020.113231
33. Brenner JS, Pan DC, Myerson JW, et al. Red blood cell-hitchhiking boosts delivery of nanocarriers to chosen organs by orders of magnitude. *Nat Commun*. 2018;9(1):2684. doi:10.1038/s41467-018-05079-7
34. Bisso PW, Gaglione S, Guimarães PPG, et al. Nanomaterial interactions with human neutrophils. *ACS Biomater Sci Eng*. 2018;4(2):4255–4265. doi:10.1021/acsbiomaterials.8b01062
35. Zheng Y, Ma L, Sun Q. Clinically-relevant ABC transporter for anti-cancer drug resistance. *Front Pharmacol*. 2021;4:12.

36. Siegal T, Horowitz A, Gabizon A. Doxorubicin encapsulated in sterically stabilized liposomes for the treatment of a brain tumor model: biodistribution and therapeutic efficacy. *J Neurosurg*. 1995;83(6):1029–1037. doi:10.3171/jns.1995.83.6.1029
37. Hao J, Chen J, Wang M, et al. Neutrophils, as "Trojan horses", participate in the delivery of therapeutical PLGA nanoparticles into a tumor based on the chemotactic effect. *Drug Deliv*. 2020;27(1):1–14. doi:10.1080/10717544.2019.1701141
38. Sun W, Xie C, Wang H, Hu Y. Specific role of polysorbate 80 coating on the targeting of nanoparticles to the brain. *Biomaterials*. 2004;4:25.